16th World Conference on Earthquake, 16WCEE 2017

Santiago Chile, January 9th to 13th 2017

Paper N° 611 (Abstract ID)

Registration Code: S-O1461743463

FORMULA FOR SHEAR STRENGTH OF CYLINDRICAL SHEAR-KEY

APPLIED SEISMIC RETROFITTING

T. Abe(1), T. Hiwatashi(2), M. Kubota(3), Y. Takase(4), K. Katori(5)

(1) *Reserch Institute of Tecnology, TOBISHIMA Corporation, Japan, takahide_abe@tobishima.co.jp*
(2) *Senior Researcher, Reserch and Development Center, TOA Corporation, Japan, t_hiwatashi@toa-const.co.jp*
(3) *Reserch Institute of Tecnology, TOBISHIMA Corporation, Japan, masaharu_kubota@tobishima.co.jp*
(4) *Associate Professor, College of Environmental Technology, Muroran Institute of Technology, Japan, y.takase@mmm.muroran-it.ac.jp*
(5) *Professor, Department of Architecture, Faculty of Science & Engineering, Toyo University, Japan, katori@toyonet.toyo.ac.jp*

Abstract

In the seismic retrofitting of an existing concrete structure, the surface of the structural frame is chipped to improve the integrity between the existing frame and retrofitting member. But, quantitatively evaluating strength of these joints are difficult because the concavo-convex shape is influenced by construction worker. Therefore, the authors developed a new joint referred to as the cylindrical shear-key. The cylindrical shear-key is made by filling a cylindrical core on the concrete surface with grout or concrete, and resists shear forces as a shear-key. Creating a uniform shape is expected to enable quantitative strength evaluation. In this study, direct shear tests were conducted using a cylindrical shear-key to investigate the fundamental performance of the shear-key. Then, based on the test results, an formula was developed for evaluating the strength of cylindrical shear-key, and it was shown that the maximum strength could be quantitatively evaluated accurately. And cylindrical shear-key is can contribute to the progression of seismic retrofitting.

Keywords: Concrete surface roughening, Bearing resistance, Shear-key, Earthquake retrofitting, Shear strength

1. Introduction

Retrofitting existing buildings with low earthquake resistance has recently been a critical issue. For improving the earthquake resistance of existing buildings using retrofitting members, it is important to ensure that the retrofitting members are integrated with the existing frame. To that end, the surface of the existing frame is generally chipped using an electric chipping hammer when a reinforced concrete structure is retrofitted, and post-installed anchors are frequently applied. Quantitative evaluation of shear strength is, however, difficult because unevenness varies depending on the skill of the construction engineer. Chipping also produces considerable noise, vibration and dust.

Against such a background, the authors started developing a new joining method that would take the place of chipping. The authors propose a joining method that involves the creation of a cylindrical depression on the surface of the existing frame (hereinafter referred to as the cylindrical shear-key) using a core drill rather than forming a depression using an electric chipping hammer. Using a core drill results in a uniform depression created regardless of the skill of the engineer, and greatly reduces the vibration, noise and dust described above. Filling the cylindrical core with grout or concrete enables the cylindrical shear-key to resist shear forces acting at the joint as a shear-key.

The objectives of this study are to conduct element tests using a cylindrical shear-key to identify its fundamental characteristics, and to develop an formula for evaluating shear strength.

2. OUTLINE OF CYLINDRICAL SHEAR-KEY

Figure 1 gives a conceptual view of shear resistance elements and mechanical behavior that the authors assume at the joint. Each resistance element is expected to exhibit different mechanical behavior [1] (Figure 1). Stiffness, deformation at the maximum strength and behavior in the post-peak area also vary. For building an appropriate design method, therefore, the mechanical behavior of each shear resistance element should be modeled thoroughly and verification should be made collectively.

Figure 2 shows the shape of cylindrical shear-key and an example of application of cylindrical shear-keys. The minimum width at the joint to which seismic retrofit is applied is approximately 200 mm. The pitch of post-installed anchor is generally around 150 mm in most cases. Then, the diameter of cylindrical shear-key *R* was set at approximately 50 mm considering the installation of a cylindrical shear-key at the midpoint between post-installed anchors. The height of cylindrical shear-key *t* was set at 5 or 10 mm.

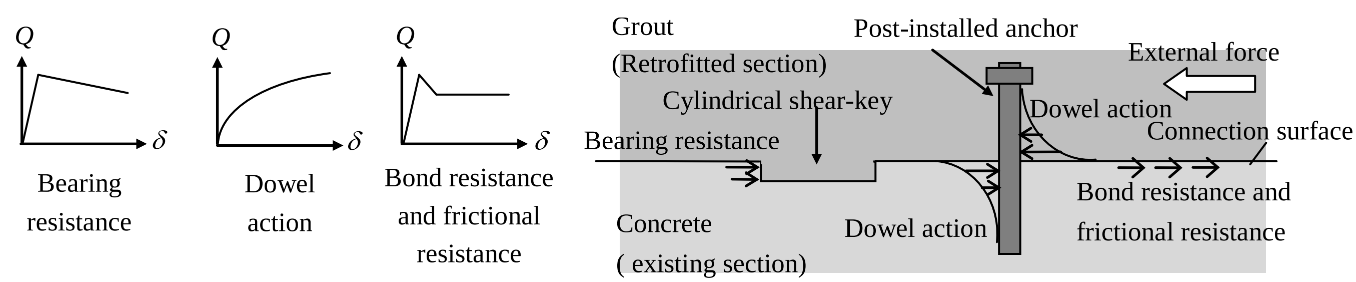

Figure 1. Concept of assumed shear resistance elements and mechanical behavior at the joint

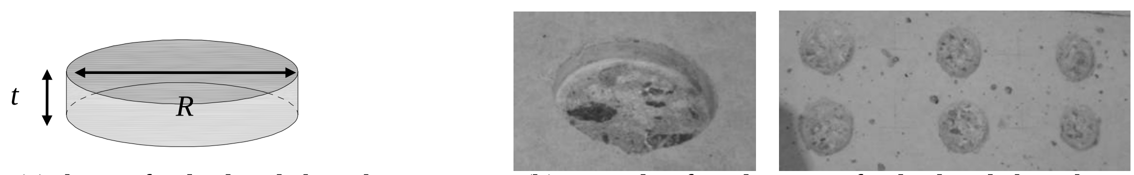

(a)Shape of cylindrical shear-key (b)Example of application of cylindrical shear-key

Figure 2. Shape and example of application of cylindrical shear-key

3. OUTLINE OF SHEAR LOADING TEST

3.1 Test parameters

Table 1 shows list of specimens. The bearing pressure that is carried by the concrete in the existing section is considered to be determined by the area subjected to the pressure and the compressive strength of the concrete in the existing section. It was also reported that in tests at the joint in a precast concrete structure, longitudinal stress affects the shear strength on the connection surface [2]. The pressure area depends on R and t. In the test, R was fixed while t was made to vary. Varying factors were therefore the width-height ratio R/t, compressive strength of concrete in the existing section ${}_C\sigma_B$ and mean compressive stress σ_0. σ_0 is longitudinal force N divided by the area of connection surface A.

$$\sigma_0 = N / A \tag{1}$$

The connection surface was coated with grease to minimize bonding resistance and frictional resistance occurring between the concrete surface and grout.

Table 1. list of specimens

Specimen		R/t	σ_0 (N/mm^2)	Concrete in existing section	
				${}_C\sigma_B$ (N/mm^2)	Young's modulus (kN/mm^2)
S1	S1-1	5.2 (R=52mm, t=10mm)	0.48	14.5	22.1
	S1-2				
S2	S2-1			32.9	27.7
	S2-2				
S3	S3-1		0.95	14.5	22.1
	S3-2				
S4	S4-1	10.4 (R=52mm, t=5mm)	0.48		
	S4-2				
S5	S5-1			32.9	27.7
	S5-2				
S6	S6-1		0.95	14.5	22.1
	S6-2				

3.2 Specimen dimensions

The dimensions of specimen are shown in Figure 3. The dimensions of the grout in the retrofitted section simulate the joint where seismic retrofitting is applied. As described earlier, cylindrical shear-keys were applied at the midpoint between post-installed anchors with an assumed pitch of 150 mm. Both the width and height were set at 200 mm based on the general cross section at the joint where seismic retrofitting was applied. The compressive strength of grout in the retrofitted section was 57.3 N/mm^2.

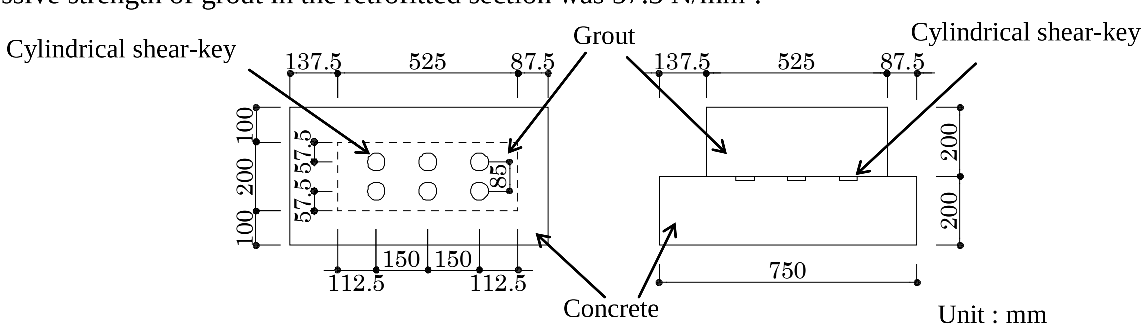

Figure 3. Dimensions of specimen

3.3 Loading and measurement

The Setup of loading test is shown in Figure 4. Loading was controlled longitudinally. Monotonous loading was applied in the horizontal direction. In order to minimize the frictional resistance created by the loading device, roller bearings were installed in two directions on the thick loading plate. Rubber sheets were placed between the thick steel plate and grout in the retrofitted section, and between the concrete in the existing section and the steel bottom plate. Thus, longitudinal compressive stress was equally distributed throughout the specimen.

For horizontal displacement, a mean of the measurements obtained using sensitive displacement gauges installed at two points between the concrete in the existing section and the grout in the retrofitted section in the longitudinal direction.

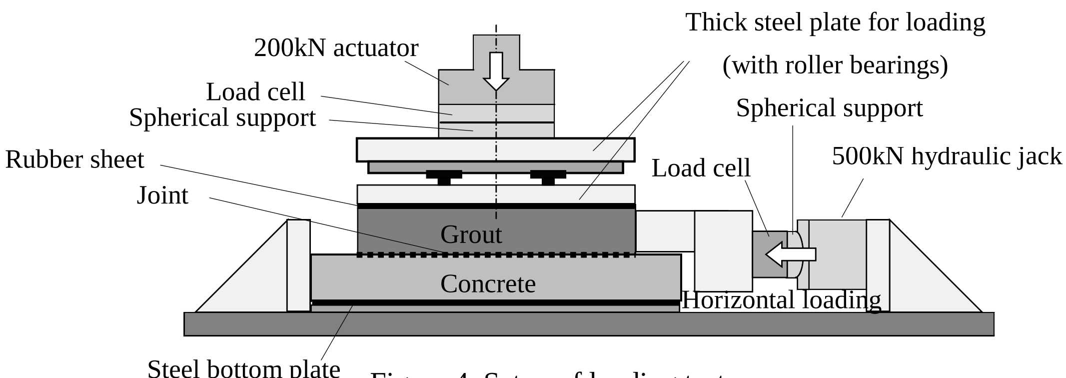

Figure 4. Setup of loading test

4. TEST RESULT

4.1 Horizontal load - displacement(Q - δ) relations

Figure 5 shows horizontal load-displacement (Q-δ) curves. No measurements were obtained in specimens S1-1, 2-1 and 2-2 because of rapid displacement after the maximum horizontal load Q_{max} was reached. In the other specimens, behavior could be measured beyond Q_{max}. It was observed that horizontal load gradually approached a certain level as horizontal displacement progressed. The difference in behavior is assumed to be ascribable to the difference in failure mode of cylindrical shear-key.

4.2 Comparison of maximum horizontal load using different varying factors

Figure 6 compares Q_{max}- R/t relations in specimens while R/t was varied. Specimens were compared with each other in the case where varying factors other than R/t were assumed to be the same. Q_{max} was greater in the specimen with smaller R/t. R/t had smaller effect in the specimen with ${}_C\sigma_B$ = 32.9 N/mm^2 than in the specimen with ${}_C\sigma_B$ = 14.5 N/mm^2. This may be because of the difference in failure mode depending on such varying factors as R/t and ${}_C\sigma_B$.

Figure 7 compares Q_{max}- ${}_C\sigma_B$ relations in specimens while ${}_C\sigma_B$ was varied. Comparison was made in the case where varying factors other than ${}_C\sigma_B$ were assumed to be the same. Q_{max} was greater in the specimen with higher ${}_C\sigma_B$. Regression coefficient was lower in the specimen with R/t = 5.2 than in the specimen with R/t = 10.4. Q_{max} was affected less by ${}_C\sigma_B$. Q_{max} was greater in the specimen with smaller R/t as described above. Failure mode in specimen S2 may therefore be different from that in other specimens.

Figure 8 compares Q_{max}- σ_0 relations in specimens while σ_0 was varied. Q_{max} was greater in the specimen with higher σ_0. The influence of σ_0 on Q_{max} was examined based on the regression coefficients of specimens with R/t = 5.2 and 10.4. The influence was generally constant regardless of R/t.

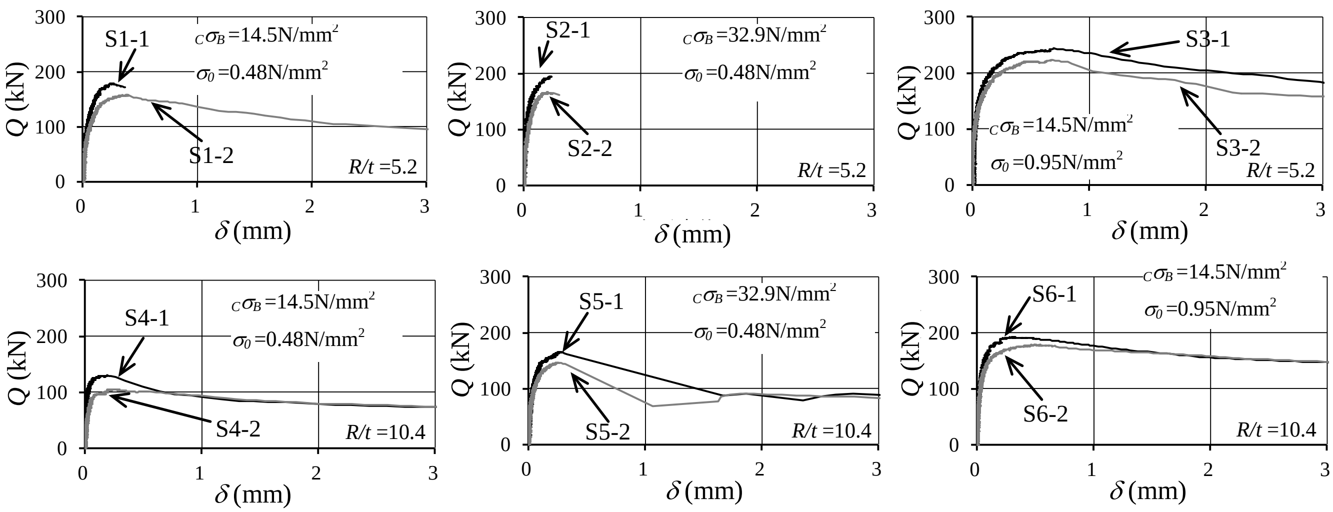

Figure 5. Horizontal load-displacement (Q-δ) curves

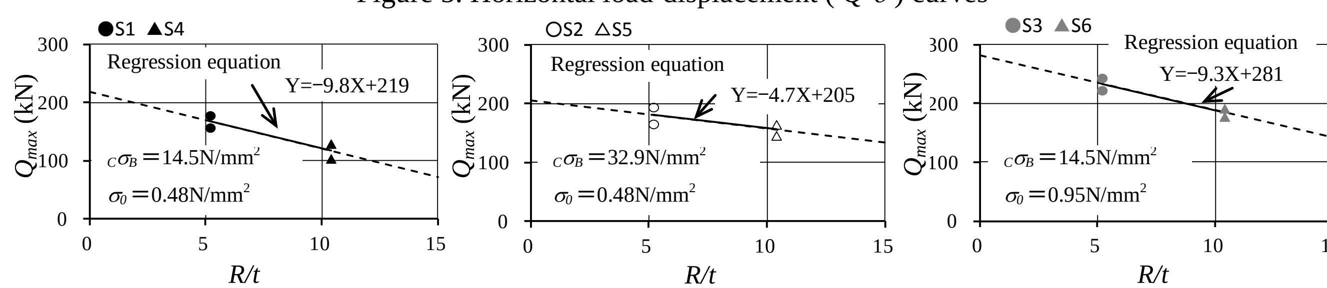

(a) S1,S4 (b) S2,S5 (c) S3,S6

Figure 6. Comparison of Q_{max} − R/t relations in specimens while R/t was varied

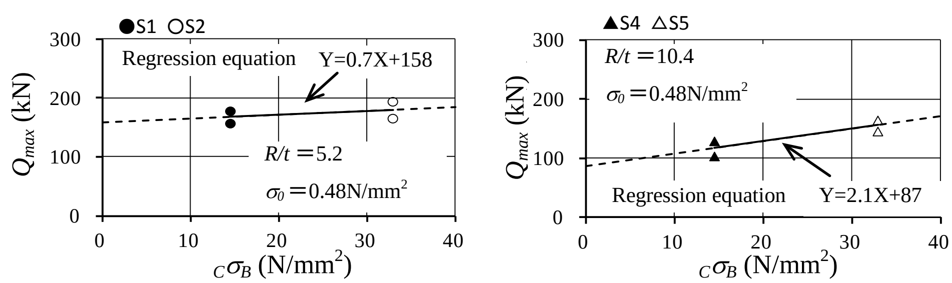

(a) S1,S2 (b)S4,S5

Figure 7. Comparison of Q_{max} − R/t relations in specimens while $_{C}\sigma_B$ was varied

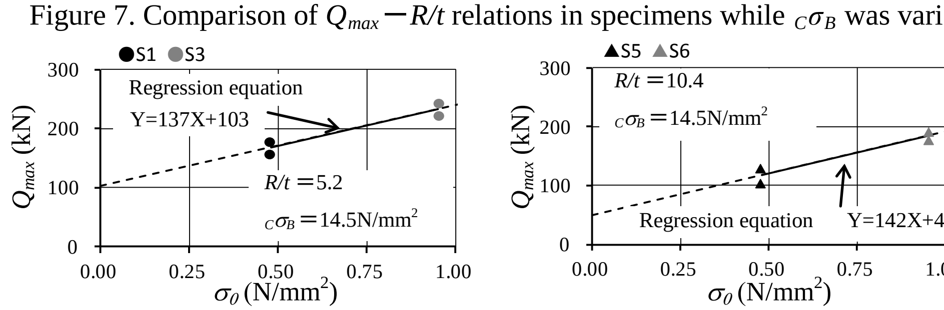

(a) S1,S3 (b)S4,S6

Figure 8. Comparison of Q_{max} − R/t relations in specimens while σ_0 was varied

4.3 Failure modes

At the end of loading, grout in the retrofitted section was separated from the concrete in the existing section, and the connection surface was observed. Three failure modes were observed. They were the bearing failure of concrete in the existing section, shear-off failure of cylindrical shear-key and composite failure involving the preceding two types (hereinafter referred to as composite failure). Figure 9 shows the failure modes. Table 2 lists the types and quantities of failure modes in each specimen. For convenience sake, the bearing failure of concrete in the existing section, composite failure and shear-off failure of cylindrical shear-key were expressed as failure modes A, B and C, respectively. Figure 10 compares frequency distributions of failure modes while different factors were varied. In order to prevent the frequency to vary, the specimens compared in Section 4.2 were compared while a different factor was varied.

Figure 10 (a) shows that when *R/t* was varied, most of the failure modes in specimens with *R/t* = 5.2 were shear-off failure of cylindrical shear-keys or composite failure, but all of the failure modes in specimens with *R/t* = 10.4 were bearing failure of concrete in existing section.

Figure 10 (b) shows that when ${}_C\sigma_B$ was varied, most of the failure modes in specimens with ${}_C\sigma_B$ = 14.5 N/mm^2 were bearing failure of concrete in existing section, but half of the failure modes in specimens with ${}_C\sigma_B$ = 32.9 N/mm^2 were shear-off failure. Shear-off failure of cylindrical shear-keys occurred exclusively in specimen S2 with ${}_C\sigma_B$ = 32.9 N/mm^2 and *R/t* = 5.2.

Figure 10 (c) compares failure modes in the case where σ_0 was varied. The frequency of bearing failures of concrete in existing section was lower and the frequency of composite failures was higher in specimens with σ_0 = 0.95 N/mm^2 than in specimens with σ_0 = 0.48 N/mm^2. The difference was, however, not outstanding as compared with the tendency of failure modes while other factors were varied as far as the test was concerned.

As a summary of the above discussions, the failure mode is likely to be the shear-off failure of cylindrical shear-keys where 5.2 or lower *R/t* and high ${}_C\sigma_B$ are specified.

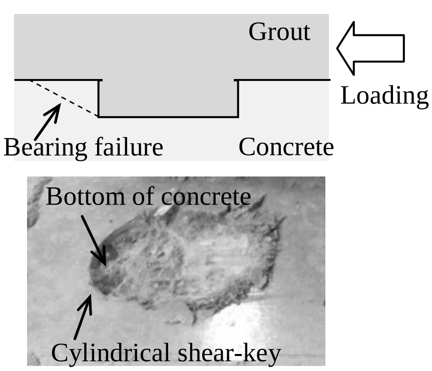

(a)Bearing failure of concrete(A)

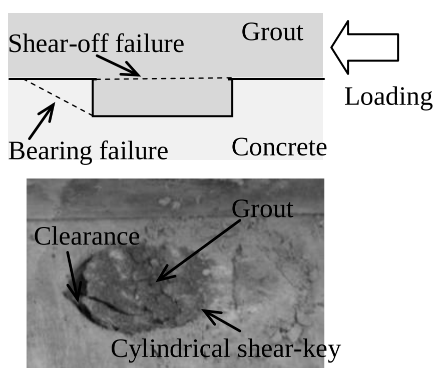

(b)Composite failure(B)

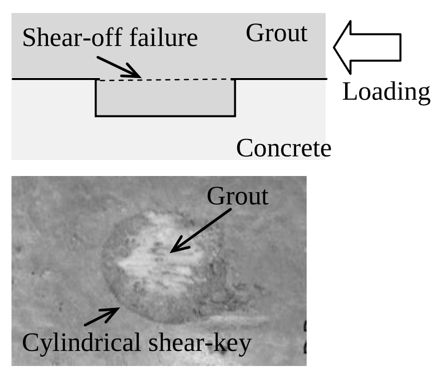

(c)Shear-off failure of cylindrical shear-key(C)

Figure 9. Failure modes

Table 2. Failure modes and their quantities in each specimen

Specimen	Failure mode and quantity			Specimen	Failure mode and quantity			Speimen	Failure mode and quantity		
	A	B	C		A	B	C		A	B	C
S1-1	3	1	2	S3-1	0	6	0	S5-1	6	0	0
S1-2	0	5	1	S3-2	0	6	0	S5-2	6	0	0
S2-1	0	0	6	S4-1	6	0	0	S6-1	6	0	0
S2-2	0	0	6	S4-2	6	0	0	S6-2	6	0	0

※Failure mode A : Bearing failure of concrete, Failure mode B : Composite failure, Failure mode C : Shear-off failure of cylindrical shear-key

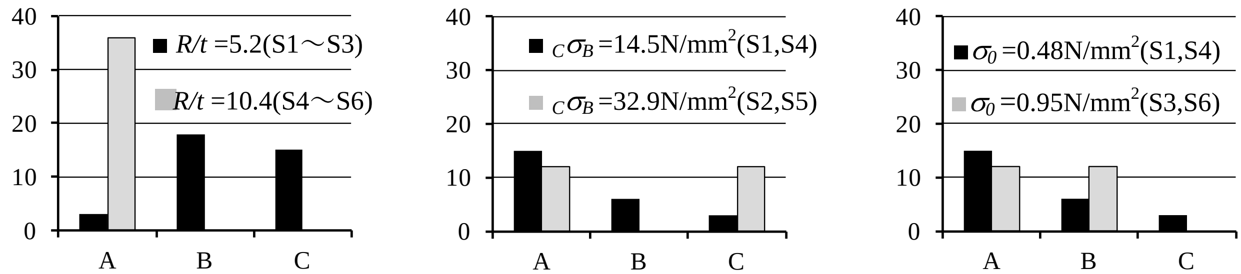

(a) R/t (b) ${}_C\sigma_B$ (c) σ_0

Figure 10. Comparison of frequency distributions of failure modes while each factor was varied

5. PROPOSE OF SHEAR STRENGTH FORMULA OF CYLINDRICAL SHEAR-KEY

5.1 Configuration of proposed shear strength formula

5.1.1 Basic shear strength formula

It is assumed that the concrete in the existing section is subjected to a bearing force of cylindrical shear-key. Existing studies [3], [4] suggest that bearing strength is correlated with the exponential of ${}_C\sigma_B$. The shear strength of cylindrical shear-key Q_{sky} is the product of multiplication of pressure area A_{sky}, bearing coefficient K and the nth power of ${}_C\sigma_B$ (formula (2)).

$$Q_{sky} = A_{sky} \cdot K \cdot {}_C\,\sigma_B{}^n \tag{2}$$

Figure 11 shows the assumed shearing resistance area of cylindrical shear-key. It is assumed in view of the state of bearing failure of concrete in the existing section that bearing stresses σ_C are distributed radially from the center of the cylindrical shear-key (Figure 11). σ_C is assumed to uniformly act circularly. If σ_C is regarded as the mean of stresses distributed in the direction of height of cylindrical shear-key although σ_C is not always distributed uniformly in the direction of the height of cylindrical shear-key, Q_{sky} corresponds to the value obtained by integrating $\sigma_C{}^S$, the element of σ_C in the direction of shear, along the arc of cylindrical shear-key and in the vertical direction (in the y direction). Then, the following formula is obtained.

$$Q_{sky} = \int_r \sigma_c \cdot \cos\theta \cdot dA_{sky} = \int_r \sigma_c^s \cdot dA_{sky} \tag{3}$$

where, θ is the angle of σ_C to the direction of shear, r is the area where σ_C acts on the arc and dA_{sky} is the minute pressure area.

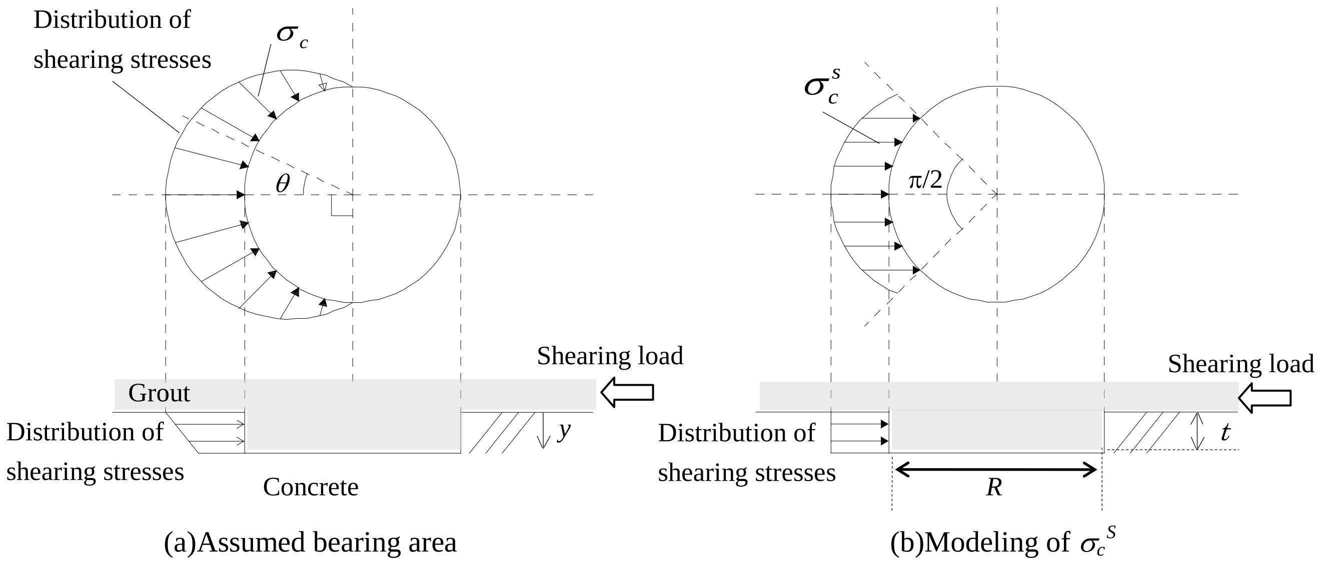

Figure 11. Assumed shearing resistance area of cylindrical shear-key

5.1.2 Pressure area

It is assumed that cylindrical shear-key resists mainly the shearing force in the area plus or minus π/4 rad. from the center of the shear key to the point where shearing force acts, and that $\sigma_C{}^S$ acts equally regardless of θ and vertical distance. Then, A_{sky} is expressed by

$$A_{sky} = \int_r dA_{sky} = \int_{-\pi/4}^{+\pi/4} t \cdot \frac{R}{2} d\theta = \frac{\pi \cdot R \cdot t}{4} \tag{4}$$

5.1.3 Bearing coefficient

It is assumed based on test results that K is composed of factors R/t, ${}_C\sigma_B$ and σ_0. Figure 12 shows a concept of vertical distribution while R/t is varied. As shown in the figure, the mean in the vertical direction is expected to be reduced if the vertical distance increases. When R remains the same, therefore, the mean in the vertical direction $\sigma_C{}^S$ increases and then K also increases as R/t increases.

As shown in formula (2), K and n are identified more easily if K or n is fixed. Thus, the authors assume $n = 1$ in formula (2) and give a term of mth power of ${}_C\sigma_B$ as a component of K. Finally, the sum of n and m was used as an exponential.

σ_0 acts vertically to the direction of shear. If σ_0 increases, the vertical deformation of concrete in existing section is restrained. As a result, K increases and finally Q_{sky} also increases.

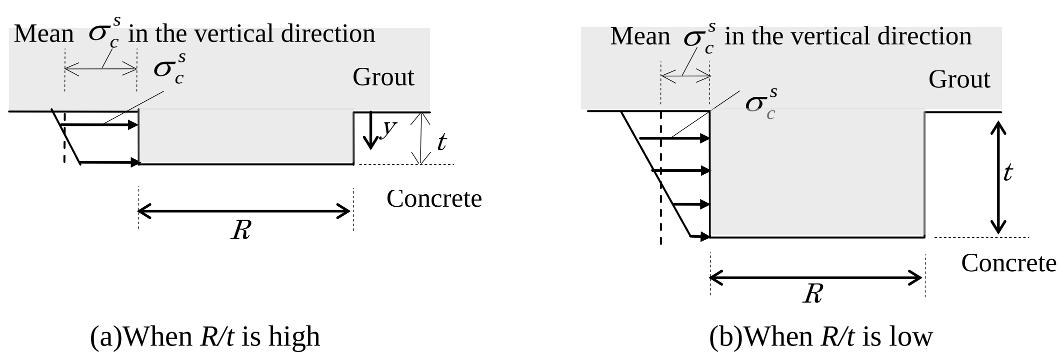

Figure 12. Concept of $\sigma_c{}^S$ vertical distributions depending on R/t

5.2 Evalution of bearing coefficient where each factor was varied

In order to evaluate K considering R/t, ${}_C\sigma_B$ and σ_0, bearing coefficient is obtained while each factor is varied and used to express K. Bearing coefficients that are identified using R/t, ${}_C\sigma_B$ and σ_0 are expressed by $K_{R/t}$, K_C *and* K_{comp}, respectively. Described below are detailed methods for identifying K. As in Section 4.3, specimens with a varying factor were selected to prevent the varying factor specified for numerous specimens from having great influences.

5.2.1 Basic bearing coefficient

In the shear strength formula, K is set considering all the varying factors. First, correction coefficients are obtained for different varying factors ($C_{R/t}$, C_C *and* C_{comp}), which are then used to obtain a standard value of bearing coefficient K' free from the influence of varying factors. Correction coefficients for different varying factors are expressed by dividing $K_{R/t}$, K_C *and* K_{comp} by the standard value of bearing coefficient for each factor (for the method for calculating the standard value, refer to the following section). The formula below shows K in the case where all the varying factors are taken into consideration.

$$K = K' \cdot C_{R/t} \cdot C_C \cdot C_{comp} = K' \frac{K_{R/t}}{K'_{R/t}} \cdot \frac{K_C}{K'_C} \cdot \frac{K_{comp}}{K'_{comp}} \tag{5}$$

where, $C_{R/t}$ is the correction coefficient for $K_{R/t}$, C_C is the correction coefficient for K_C, C_{comp} is the correction coefficient for K_{comp}, $K'_{R/t}$ is the standard value of $K_{R/t}$, K'_C is the standard value of K_C and K_{comp} is the standard value of K'_{comp}.

Regression equations for $K_{R/t}$ and K_{comp} are assumed to be least squares linear functions and regression function for K_C was assumed to be a least squares exponential function. Then, $K_{R/t}$, K_C and K_{comp} for each varying factor could be given by

$$K_{R/t} = A_{R/t} \cdot R/t + B_{R/t} \tag{6}$$

$$K_C = D_C \cdot {}_C\sigma_B{}^m \tag{7}$$

$$K_{comp} = A_{comp} \cdot \sigma_0 + B_{comp} \tag{8}$$

where, $A_{R/t}$ is the regression coefficient of $K_{R/t}$, A_{comp} is the regression coefficient of K_{comp}, $B_{R/t}$ is the constant term of $K_{R/t}$, B_{comp} is the constant term of K_{comp} and D_C is a coefficient.

Based on formulas (2), (5) and (7), Q_{sky} is expressed by formula (9) using ${}_C\sigma_B$.

$$Q_{sky} = A_{sky} \cdot K' \cdot C_{R/t} \cdot C_{comp} \frac{D_C \cdot {}_C\sigma_B{}^{(m+n)}}{K'_C} \tag{9}$$

5.2.2 Setting of bearing coefficient

Figure 13 shows distributions of bearing coefficients while different factors are varied. Bearing coefficients while different factors are varied $K_{R/t}$, K_C and K_{comp} can be obtained using the following formula.

$$K_p = \frac{Q_{\max}}{A_{sky} \cdot {}_C\sigma_B{}^n} \tag{10}$$

Subscript p in K_p corresponds to the varying factors (*R/t*, *C* and *comp*) shown in formulas (5) through (8). n is set to be 1 as described in Section 5.1.1. The values of constants in formulas (6) through (8) are as shown in regression equations in Figure 13.

In the test, two varying factors were specified at a time. The standard value of each varying factor for obtaining the correction coefficient can be obtained by substituting the mean of each varying factor in formulas (6) through (8). Each standard value can be formulated by

$$K'_{R/t} = A_{R/t} \cdot \overline{R/t} + B_{R/t} \tag{11}$$

$$K'_C = D_C \cdot {}_C\overline{\sigma}_B^m \tag{12}$$

$$K'_{comp} = A_{comp} \cdot \overline{\sigma}_0 + B_{comp} \tag{13}$$

where, $\overline{R/t}$ is the mean of R/t 's that were used in the test, ${}_C\overline{\sigma_B}$ is the mean of ${}_C\sigma_B$'s used in the test, and $\overline{\sigma_0}$ is the mean of σ_0's used in the test.

Based on the correction coefficients obtained using the above parameters, the standard value of bearing coefficient ${}_iK'$ for each specimen was obtained. The mean of the standard values ${}_iK'$ was defined as K'. K' was 4.844.

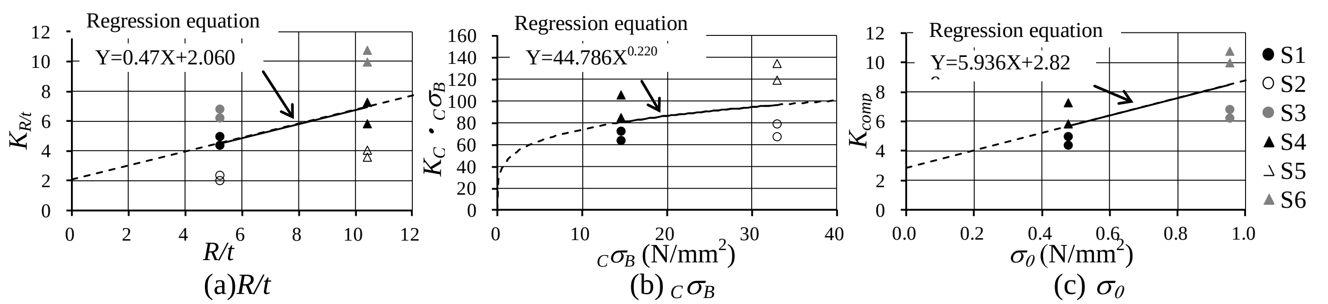

Figure 13. Distributions of bearing coefficients while different factors are varied

5.3 Comparison between test and calculated values

Table 7 lists safety factors obtained in testing and by calculation. Figure 14 shows comparison of test and calculated values. The calculated values could reproduce the values obtained in the test with a precision of plus or minus 20%. The correlation coefficient was 0.93. Thus a high precision was achieved. In this study, test values were evaluated using a single strength formula regardless of the failure mode. As a result, it was determined that the proposed formula could properly reproduce test results.

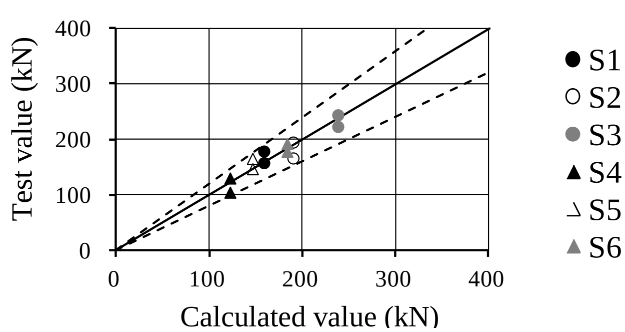

Figure 14. Comparison of test and calcurated values

6. CONCLUSIONS

The authors proposed cylindrical shear-keys that enable the evaluation of shear strength by creating uniform depressions as a means of bonding instead of chipping, and verified their structural performance. Shear strength of cylindrical shear-key was also formulated. The knowledge obtained in this study is described below.

1) As a result of direct shear tests, it was found that greater maximum horizontal load Q_{max} was obtained where width-height ratio R/t was lower and compressive strength of concrete in the existing section ${}_C\sigma_B$ and mean compressive stress σ_0 were higher.

2) In the case where ${}_C\sigma_B$ was high at 32.9 N/mm^2 and R/t was low at 5.2, the failure mode was shear-off failure. Conversely, in the case where R/t was set to be 10.4, the failure mode was exclusively the bearing failure of concrete in the existing section regardless of other conditions (although ${}_C\sigma_B$ ranged from 14.5 to 32.9 N/mm^2 and σ_0 from 0.48 to 0.95 N/mm^2).

3) A shear strength formula was developed where R/t, ${}_C\sigma_B$ and σ_0 were taken into consideration. It was shown that Q_{max} obtained in the test could be estimated highly accurately with a precision of plus or minus 20% and a correlation coefficient of 0.94.

5. References

[1]Katori, K., Hayashi, S., and Norimono, T. (1999). Influence of form and plural arrangement of shear key put on precast joint of its shear characteristics. *Journal of Structural Construction Engineering*., AIJ. No518:71-78

[2]Mochizuki, S., Makitani, E., and Nagasaka, T. (1991). Ultimate shear strength of vertical connections between precast concrete wall panels. *Journal of Structural Construction Engineering*., AIJ. No424:11-22

[3]Nakano, K., and Matsuzaki, Y. (2001).Additional method of shear resistances in precast concrete connections. *Journal of Structural Construction Engineering*., AIJ. No572:111-116

[4] Ollgaard, J. G., Slutter, R. G. and Fisher, J. W. (1971). Shear strength of stud connectors in lightweight and normal-weight concrete. *AISC Eng.Journal*: 55-64